PERGAMON

Engineering Fracture Mechanics 62 (1999) 497–510

Engineering Fracture Mechanics

A new singular boundary element for crack problems Application to bolted joints

H. Kebir[a,*], J.M. Roelandt[a], J. Foulquier[b]

[a]*Laboratoire de Génie Mécanique pour les Matériaux et les Structures, URA 1505, Université de Technologie de Compiègne, BP 649, 60206, Compiègne, France*

[b]*AEROSPATIALE, Centre Commun de recherches Louis-Blériot, 12 rue Pasteur, BP 76, 92152, Suresnes, Cedex, France*

Received 6 July 1997; received in revised form 18 December 1998; accepted 11 January 1999

Abstract

The present paper is concerned with the effective numerical implementation of the two-dimensional Dual Boundary Element Method to analyse the mixed-mode crack growth in bolted joints. All the boundaries are discretized with discontinuous quadratic boundary elements and the crack-tip is modeled by singular elements that exactly represent the strain field singularity $1/\sqrt{r}$. The Stress Identity Factors can be computed very accurately from the crack opening displacement at collocation points extremely close to the crack tip. Furthermore, the analysis of two-dimensional elastic contact problems is developed, with an iterative procedure. The contact equations are written explicitly with both transactions and displacements retained as unknowns. The computed results show that the proposed approach for Stress Intensity Factors evaluation is simple, produces very accurate solutions and has little dependence on the size of the elements near the crack tip. The algorithm is applied to several two-dimensional examples and the results obtained are in very good agreement with analytical solutions and experimental results carried out at the AEROSPATIALE Research Centre.

Keywords: Dual boundary element method; Singular element; Fracture mechanics; Crack propagation; Contact

1. Introduction

The Dual Boundary Element Method is a well established numerical technique to study linear elastic fracture mechanic problems [1,2,7,8], and one of the important fields

* Corresponding author. Tel.: +33-44-23-45-52; fax: +33-44-23-46-89.
E-mail address: hocine.kebir@utc.fr (H. Kebir)

0013-7944/99/$ - see front matter
PII: S0013-7944(99)00008-9

of research in fracture mechanics is the study of different procedures for the evaluation of the stress and displacement fields near the tip of a crack and in particular of the Stress Intensity Factor (SIF) [9]. In this paper the SIF are computed from the crack opening displacements at nodes of a singular element that exactly reproduces the strain field singularity $1/\sqrt{r}$. The improper integrals, that arise in the dual integral equations, are handled analytically.

Furthermore, the analysis of two-dimensional elastic contact problems is developed. The load is applied in one total step and a performing iteration method is applied. The contact equations are written explicitly with both tractions and displacements retained as unknowns [4,6].

We have applied them to study several examples: the first one shows the accuracy and stability of the singular element, and the two others concern its application to bolted joint crack problems.

2. Dual boundary integral equations

The dual equations, on which the DBEM is based, are the displacement and the traction boundary integral equations. In the absence of body forces, the boundary integral representation of the displacement components u_i, at a boundary point P, not on crack surfaces, is given by

$$C_{ij}(P)u_j(P) + \int_{\partial\Omega} T_{ij}(P,Q)u_j(Q)\ \mathrm{d}s(Q) = \int_{\partial\Omega} U_{ij}(P,Q)t_j(Q)\ \mathrm{d}s(Q) \tag{1}$$

where i and j denote Cartesian components; $T_{ij}(P,\ Q)$ and $U_{ij}(P,\ Q)$ represent the Kelvin traction and displacement fundamental solutions, respectively, at a boundary Q.

The stress components σ_{ij} are obtained by differentiation of Eq. (1), followed by the application of Hooke's law; they are given by (when $C_{ij} = \frac{1}{2}\delta_{ij}$):

$$\frac{1}{2}\sigma_{ij}(P) + \int_{\partial\Omega} S_{ijk}(P,Q)u_k(Q)\ \mathrm{d}s(Q) = \int_{\partial\Omega} D_{ijk}(P,Q)t_k(Q)\ \mathrm{d}s(Q) \tag{2}$$

and the traction components, t_j, are given by

$$\frac{1}{2}t_j(P) + n_i(P)\int_{\partial\Omega} S_{ijk}(P,Q)u_k(Q)\ \mathrm{d}s(Q) = n_i(P)\int_{\partial\Omega} D_{ijk}(P,Q)t_k(Q)\ \mathrm{d}s(Q) \tag{3}$$

where n_i denotes the ith component of the unit outward normal to the boundary, at point P. If P is on the crack surfaces the displacement equation becomes:

$$\frac{1}{2}u_i(P^+) + \frac{1}{2}u_i(P^-) + \int_{\partial\Omega} T_{ij}(P^+,Q)u_j(Q)\ \mathrm{d}s(Q) = \int_{\partial\Omega} U_{ij}(P^+,Q)t_j(Q)\ \mathrm{d}s(Q) \tag{4}$$

and the traction equation becomes:

$$\frac{1}{2}t_i(P^+) + \frac{1}{2}t_i(P^-) + n_i(P^+)\int_{\partial\Omega} S_{ijk}(P^+,Q)u_k(Q)\ \mathrm{d}s(Q) = n_i(P^+)\int_{\partial\Omega} D_{ijk}(P^+,Q)t_k(Q)\ \mathrm{d}s(Q) \tag{5}$$

3. Singular element

The crack tip is modeled by singular elements that exactly represent the strain field singularity $1/\sqrt{r}$. The nodes are positioned at $\xi = -2/3$, $\xi = 0$ and $\xi = 2/3$. The shape functions of this element are:

$$N_1(\xi) = \frac{3}{2}\,\frac{(3-\sqrt{15})\xi + 2\sqrt{1+\xi} - 2}{\sqrt{15}+\sqrt{3}-6}$$

$$N_2(\xi) = \frac{3(\sqrt{15}-\sqrt{3})\xi - 12\sqrt{1+\xi} + 2(\sqrt{15}+\sqrt{3})}{2(\sqrt{15}+\sqrt{3}-6)}$$

$$N_3(\xi) = \frac{3}{2}\,\frac{(\sqrt{3}-3)\xi + 2\sqrt{1+\xi} - 2}{\sqrt{15}+\sqrt{3}-6} \tag{6}$$

The displacement at the collocation points M_l ($l = 1, 3$) of the singular element are:

$$u_i(\xi) = \sum_{l=1}^{3} u_i(M_l)N_l(\xi) \quad (i = 1,2) \tag{7}$$

This formulation represents exactly the strain field singularity:

$$\frac{\partial u_i}{\partial \xi}(\xi = -1) = \frac{\partial \Sigma_{l=1}^{3} u_i(M_l)N_l(\xi)}{\partial \xi}(\xi = -1) = \sum_{l=1}^{3} u_i(M_l)\frac{\partial N_l(\xi)}{\partial \xi}(\xi = -1) = \infty \tag{8}$$

because

$$\frac{\partial N_l}{\partial \xi}(\xi = -1) = \infty \tag{9}$$

The improper integrals, that arise in the dual integral equations, are handled analytically [3]

$$\int_{\Gamma_s} T^i_j(P,Q)N_l(\xi)\ \mathrm{d}\xi(Q) \qquad \int_{\Gamma_s} S^i_{jk}(P,Q)N_l(\xi)\ \mathrm{d}\xi(Q) \tag{10}$$

where Γ_s is the singular element.

4. The stress intensity factor evaluation

There are several approaches to compute SIF using a dual boundary element formulation. In the present work, they are computed from the crack opening displacements at nodes which are extremely close to the tip [3].

$$K_I = \frac{\mu}{\kappa+1}\sqrt{\frac{\pi}{l}}\left[5(u_2^{N_2} - u_2^{M_2}) - \frac{3\sqrt{15}}{5}(u_2^{N_3} - u_2^{M_3})\right] \tag{11}$$

and

$$K_{II} = \frac{\mu}{\kappa+1}\sqrt{\frac{\pi}{l}}\left[5(u_1^{N_2} - u_1^{M_2}) - \frac{3\sqrt{15}}{5}(u_1^{N_3} - u_1^{M_3})\right] \tag{12}$$

where μ is the shear modulus and $\kappa = 3-4\eta$; for plane strain $\eta = \nu$ and for plane stress $\eta = \nu/(1+\nu)$, where ν is the Poisson ratio.

5. Contact algorithm

The contact constraints are exactly imposed along the interface without the introduction of additional variables since the overall equations are written in terms of tractions and displacements. This approach involves the coupling of the overall matrix equations via the appropriate contact conditions at the common interface of the contacting bodies, thus satisfying compatibility and equilibrium for the node pairs on each element pair. The load is applied in one total step and a performing iteration method is applied until stick and slip areas are found and satisfied [6].

In the first iteration, the contacting surfaces are assumed to be perfectly glued to each other, in this case the compatibility and the equilibrium equations are:

$$u_i(A) = u_i(B), \quad t_i(A) = -t_i(B), \quad i = 1,2 \tag{13}$$

The slip model follows Coulomb's law of limiting friction which is given as

$$| t_t | \leq \mu | t_n | \tag{14}$$

where the subscripts t and n refer to the local tangential and normal directions, respectively. The ratio of the tangential to the normal is calculated; if the absolute value of this ratio exceeds the coefficient of friction μ, the affected nodes are allowed to slip in the next iteration.

Finally, the normal stress at all nodes within the contact zone must be compressive for contact to be maintained. Therefore, nodes with normal tensile stresses are deleted from the contact area in the next solution stage.

6. Crack modeling strategy

The general modeling strategy, can be summarized as follows [7]:

- all boundaries are modeled with discontinuous quadratic elements, except the crack tip which is modeled by a singular element;
- the displacement Eq. (4) is applied for collocation on one of the crack surfaces;
- the traction Eq. (5) is applied for collocation on the crack surfaces;
- the displacement Eq. (1) is applied for collocation on all non-crack boundaries;
- an efficient automatic iterative scheme without load incrementation is employed in the algorithm to handle the contact iterations;
- the SIF are computed from the Crack Opening Displacement at collocation points of the singular element;
- the new crack-extension increment is modeled with new singular boundary elements. They will generate new equations and update the ones already existing with new unknowns [3].

7. Numerical results

7.1. Rectangular plate with a central slant crack

Consider a rectangular plate with an inclined central crack as shown in Fig. 4.

The plate is under the effect of a uniform traction at two opposite sides $\sigma = 100$ MPa. The crack has a length $2a$ and it is inclined 45° with respect to the plate sides. The ratio between

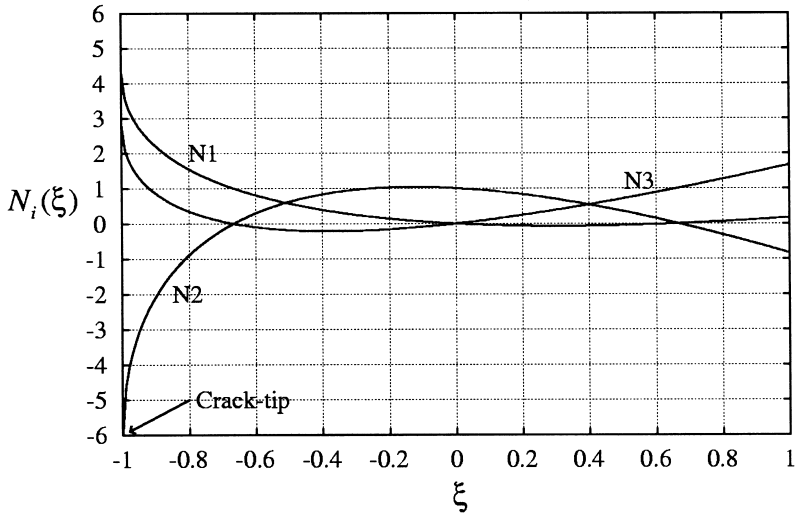

Fig. 1. Shape functions of a singular element.

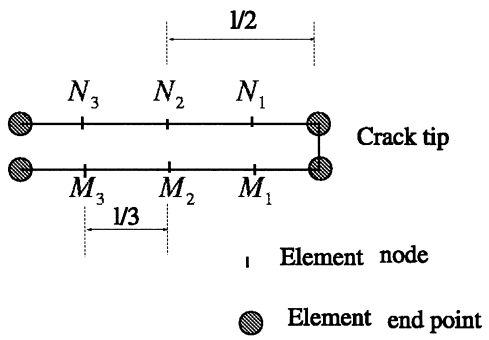

Fig. 2. Crack-tip element.

the crack length and the plate width is 0.6. The BE discretization consist of 34 quadratic elements on the external boundary. The crack discretization consists of $2N$ elements with the same length $L = a/N$.

The results obtained with the singular element are compared with those obtained with the displacement extrapolation of a quadratic element and J-integral method in Table 1 for the mode-I and mode-II SIF.

Fig. 5 shows the percentage difference with respect to Murakami's solution [5]. It can be seen in the figure that the values computed using the proposed approach have a high level of accuracy and they are stable as N varies.

7.2. Rectangular plate with four cracks

Consider now, a rectangular plate with four cracks represented in Fig. 6. The initial crack lengths are: $a_1 = 5.058$ mm, $a_2 = 5.032$ mm, $a_3 = 5.190$ mm and $a_4 = 5.095$ mm. The plate is subjected to the action of cyclical traction between σ_{max} and $R\sigma_{max}$, in which

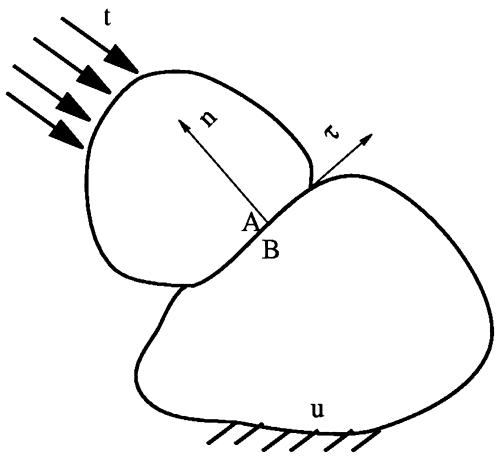

Fig. 3. Two bodies in contact.

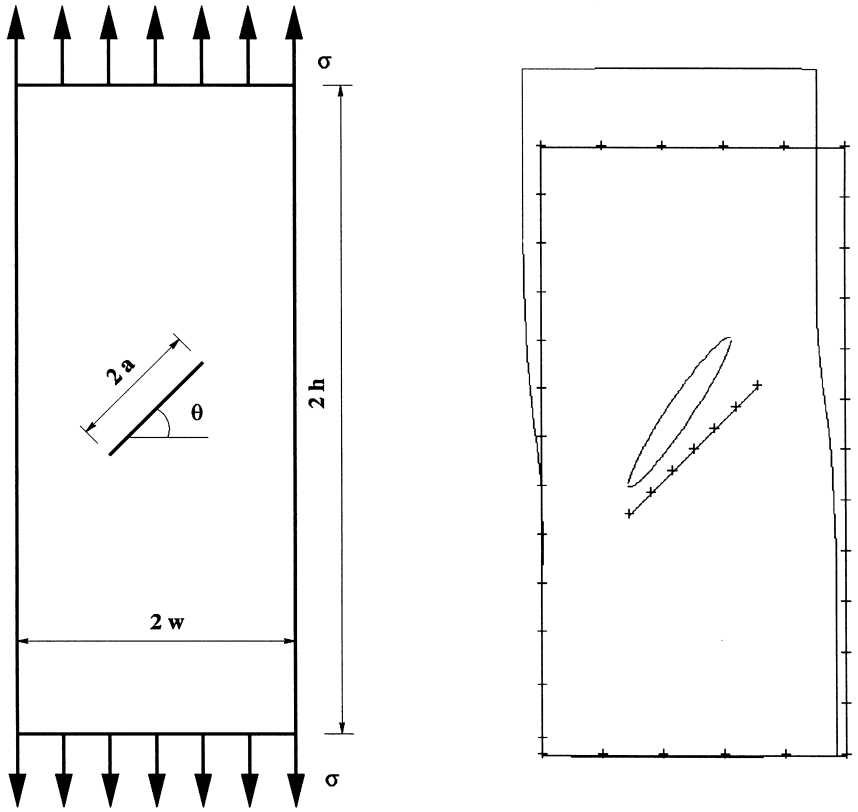

Fig. 4. Initial and deformed boundary element meshes for the centre-crack problem.

$$R = \frac{K_{\min}}{K_{\max}} = \frac{\sigma_{\min}}{\sigma_{\max}} = 0.1 \tag{15}$$

is the stress amplitude ratio of the loading cycle.

The number of loading cycles required to extend the crack a given increment is evaluated by integration of the generalized Paris model:

$$\frac{\mathrm{d}a}{\mathrm{d}N} = C(\Delta K)^n \tag{16}$$

Table 1
SIF for a rectangular plate with an inclined central crack

	Quadratic element [8]	Integral-J [8]	Singular element	Ref. [5]
K_I	0.686	0.666	0.6609	0.661
K_{II}	0.579	0.560	0.5660	0.567

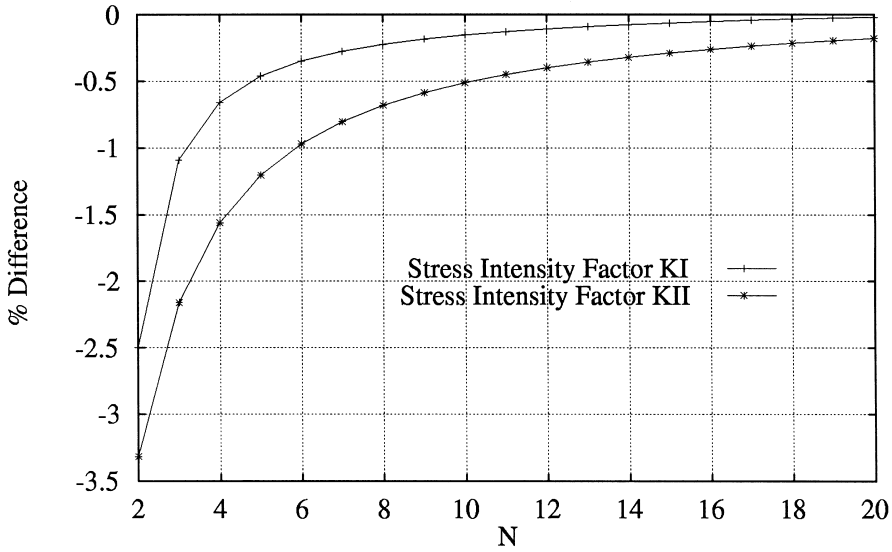

Fig. 5. Difference (percentage) of the computed SIF with Murakami's solution.

where a is the crack length, N is the number of load cycles, $K^2 = K_I^2 + 2\ K_{II}^2$, C and n are material dependent constants; in the present experience $C = 1.925 \times 10^{-7}$ and $n = 2.85$.

Experimental and numerical fatigue-life diagrams are presented in Figs. 7–9. The numerical results are obtained with 30 crack-extension increments. The difference between the

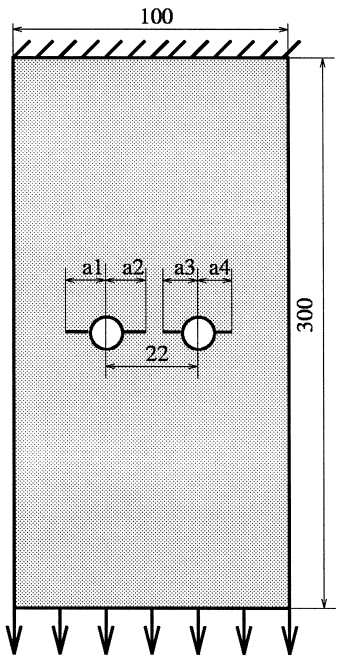

Fig. 6. Rectangular plate with four cracks.

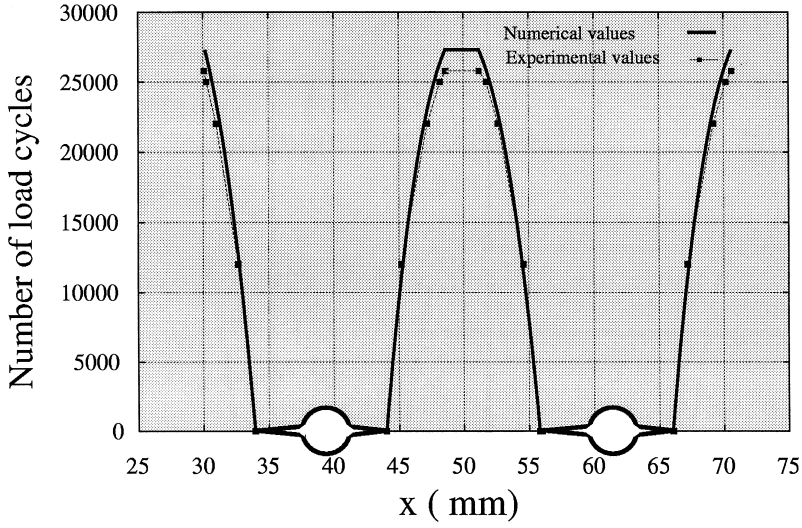

Fig. 7. Fatigue-life diagram for a rectangular plate with four cracks.

experimental results and numerical ones does not exceed 5 per cent. The CPU time is less than 120 s on DEC Alpha 500 (400 MHz).

7.3. Bolted joint with one oversized bolt

Let us consider the analysis of a bolted joint consisting of three 2024 T351 plates connected together with an oversized bolt as shown in Fig. 10.

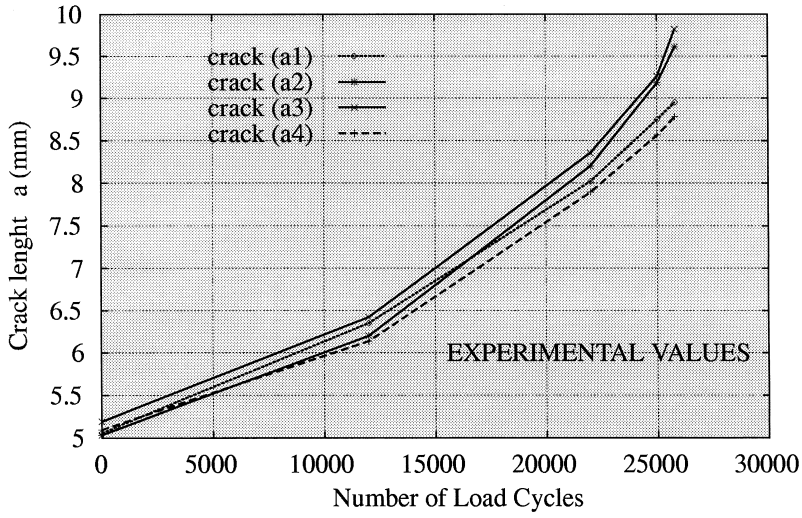

Fig. 8. Fatigue-life diagram (experimental values).

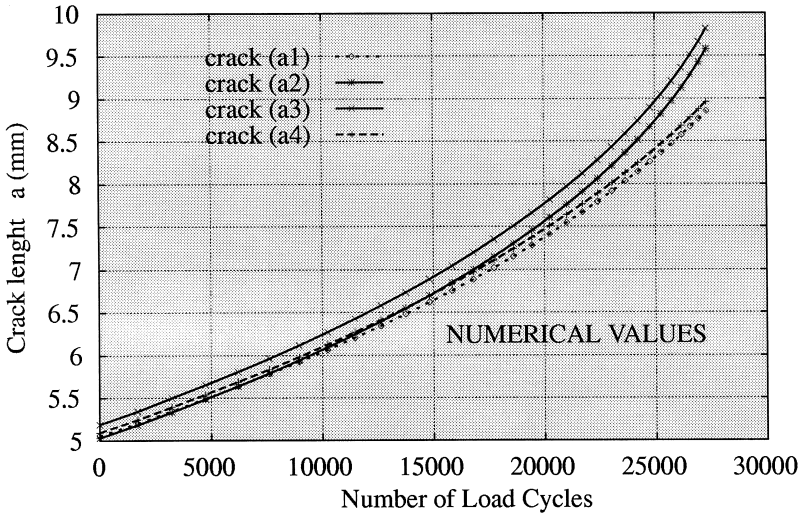

Fig. 9. Fatigue-life diagram (numerical values).

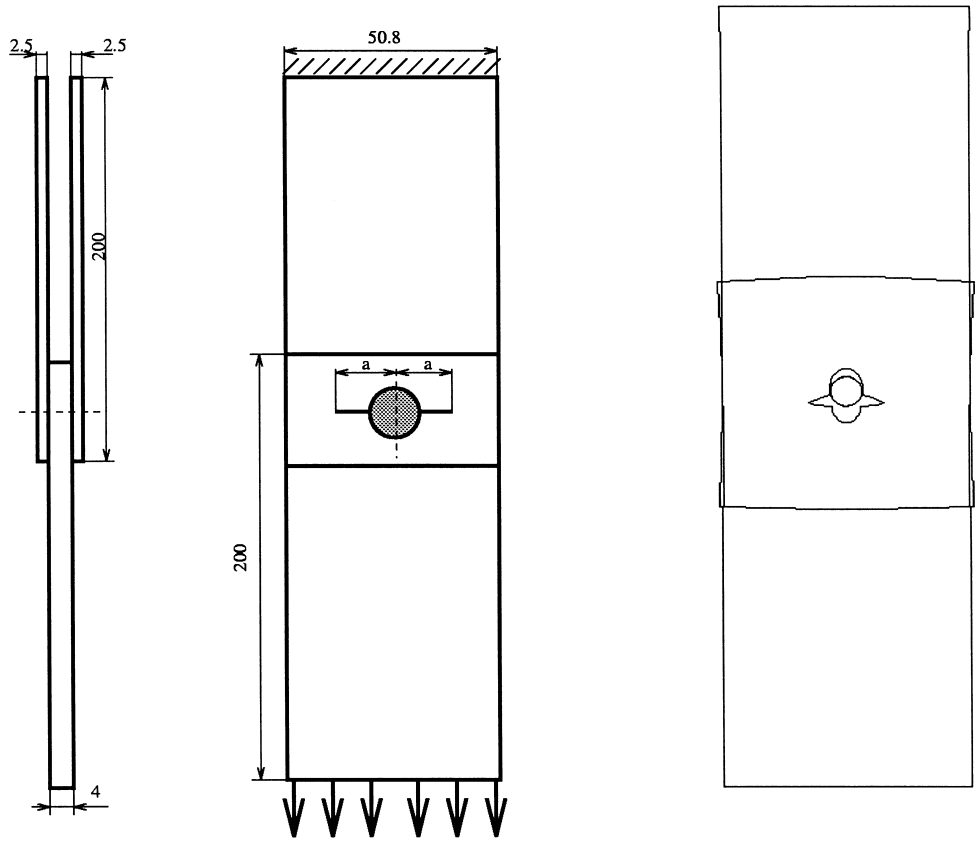

Fig. 10. Initial and deformed boundary element meshes for a bolted joint with one oversized bolt.

Crack growth tests were carried out at AEROSPATIALE Research Centre under $R=0.1$ constant amplitude loading at a frequency of 15 Hz ($\sigma_{max}=54$ MPa). Initial cracks were introduced in the central plate and three evolutions with the number of loading cycles were measured using an optical microscope (after disassembling the joint). From the corresponding crack growth rate da/dN, the experimental evaluation of ΔK with the crack length a was determined using the material Paris crack growth relation for the aluminium alloy studied, $C=2.98\times10^{-7}$ and $n=2.56$.

In Fig. 11, the experimental variation of the normalized stress intensity factor is compared to the predictions of the analytical and experimental results. Only the case of a joint with no clamping force is considered. The analytical model concerns two diametrically opposed cracks around a loaded hole [10]. The stress intensity factor is given by:

$$K=\alpha\sigma_m\sqrt{\pi a} \tag{17}$$

where

$$\sigma_m=\frac{P}{2re} \tag{18}$$

is the Caulking stress, P the hole load, e the plate thickness, $2r$ the hole diameter and a is the crack length.

Note that for a large crack the analytical model does not take into consideration the edge effect, however, it is an acceptable model for small values of crack length (although it does not

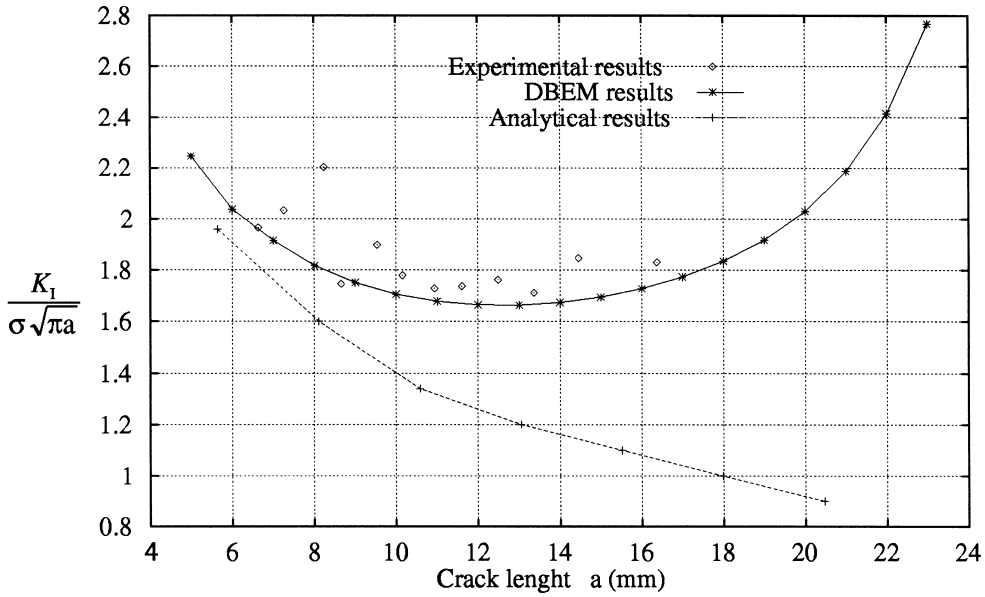

Fig. 11. Variation of normalized stress intensity factors with crack lengths.

take into consideration the contact effect). Also note that the results given by the DBEM are in good agreement with the experimental values.

7.4. Bolted joint with ten oversized bolts

As a final test, let us consider the analysis of a bolted joint consisting of three aluminium alloy plates (2024 T351) connected together with ten oversized bolts, as shown in Fig. 12.

Crack growth tests were carried out at AEROSPATIALE Research Centre under $R=0.1$ constant amplitude loading at a frequency of 10 Hz ($\sigma_{max}=100$ MPa). Initial cracks were introduced in the central plate and their evolutions with the number of loading cycles were measured using an optical microscope (after disassembling the joint). From the corresponding crack growth rate da/dN, the experimental evaluation of ΔK with the crack length a was determined using (16). For the aluminium alloy studied, $C=2.05\times10^{-8}$ and $n=3.61$.

In Fig. 13, the experimental variation of the normalized stress intensity factor is compared to

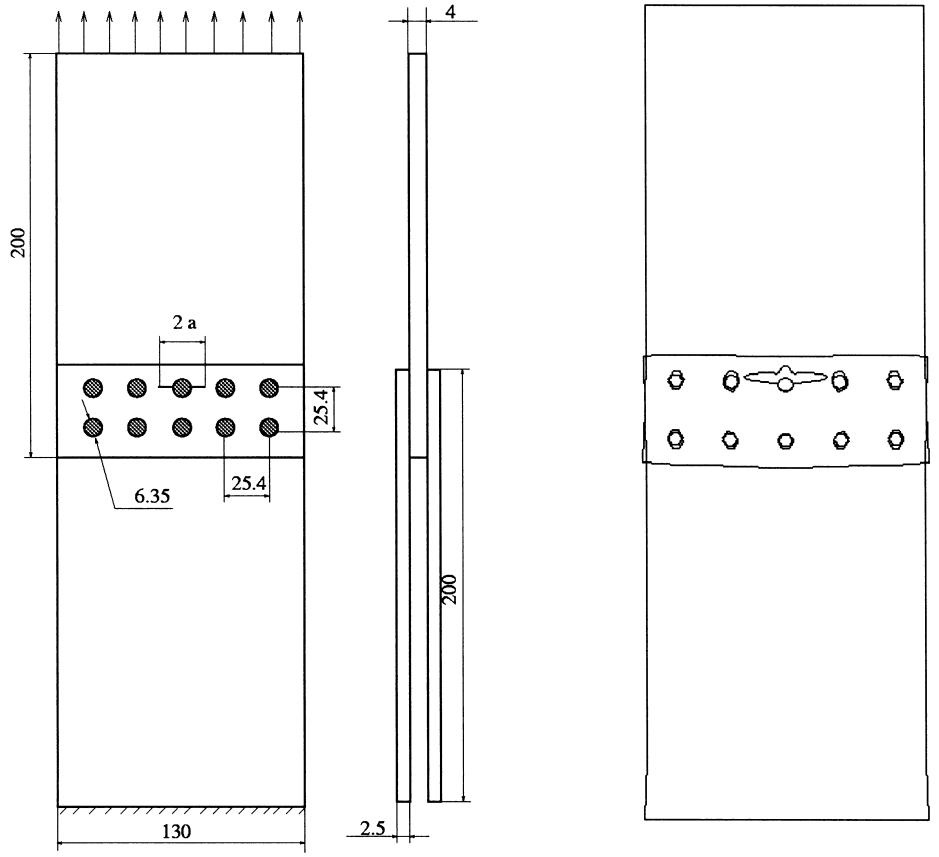

Fig. 12. Initial and deformed boundary element meshes for the bolted joint with ten oversized bolts.

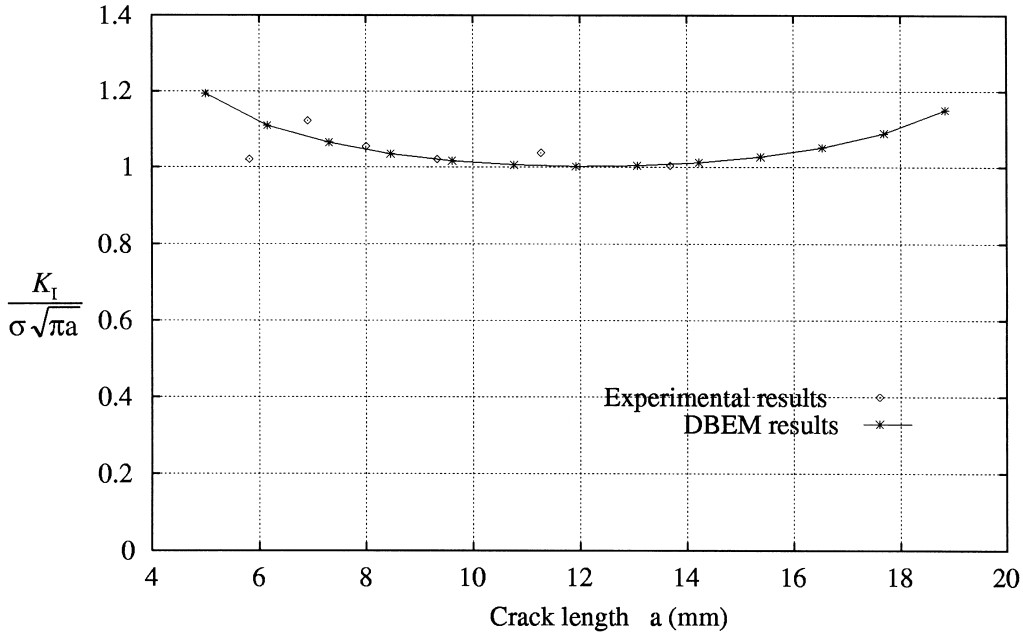

Fig. 13. Variation of normalized SIF with crack lengths.

those carried out with the dual boundary method. Note that the results given by the DBEM are in good agreement with the experimental values.

8. Conclusions

In this paper, the Dual Boundary Element Method is applied to the incremental linear elastic analysis of the crack-extension in bolted joints. For each increment of the crack extension, a stress analysis of the structure is carried out and the SIF are evaluated from the crack opening displacement at collocation points of the singular elements. This basic computational cycle is repeated for each crack extension in the direction determined by the maximum principal stress criterion. Furthermore, the analysis of two-dimensional elastic contact problems is developed with an iterative procedure. The contact equations are written explicitly with both tractions and displacements retained as unknowns.

The computed results show that the proposed approach for SIF evaluation is simple, produces very accurate solutions and has little dependence on the size of the elements near the crack tip. The algorithm is applied to several two-dimensional examples and the results obtained are in very good agreement with analytical solutions and experimental results carried out at the AEROSPATIALE Research Centre.

This simple and accurate SIF evaluation approach can also be used for dynamic crack problems and for the prediction of multiple crack linkup.

References

[1] Brebbia CA, Dominguez J. Boundary elements: an introductory course, 1st ed. New York: McGraw-Hill, 1989.
[2] Hong H, Chen J. Derivations of integral equations of elasticity. J Engng Mech 1988;114:1028–44.
[3] Kebir H, Roelandt JM. Modélisation de structures multi-fissuées par éléments de frontière singuliers. Actes du 5eme Colloque Maghrébin sur les Modèles Numériques de l'Ingénieur 1995;2:577–82.
[4] Kebir H, Roelandt JM, Foulquier J. Dual boundary element incremental analysis of crack growth in bolted joints. In: Mat-Tec96 Improvement of materials, 1996. p. 223–30.
[5] Murakami Y. Stress intensity factors handbook, 1st ed. Oxford: Pergamon Press, 1987.
[6] Olukoko OA, Becker AA. A new boundary element approach for contact problems with friction. International Journal for Numerical Methods in Engineering 1993;36:2625–42.
[7] Portela A. Dual boundary element analysis of crack growth, topics in engineering, 1st ed. Southampton and Boston, 1993.
[8] Portela A, Aliabadi MH. The dual boundary element method: effective implementation for crack problems. International Journal for Numerical Methods in Engineering 1992;33:1269–87.
[9] Saez A, Gallego R, Dominguez J. Hypersingular quarter-point boundary elements for crack problems. International Journal for Numerical Methods in Engineering 1995;38:1681–701.
[10] Shah RC. Stress intensity factors for through and part-through cracks originating at fastener holes. In: Mechanics of crack growth. ASTM, 1976. p. 590.